Applying an Improved Square Root Unscented Kalman Filtering in Tomographic Projections of Agricultural Soil Samples

MARCOS A. M. LAIA[1], PAULO E. CRUVINEL[2]

[1]Instituto de Física de São Carlos, Universidade de São Paulo - marcoslaia@gmail.com

[2]Embrapa Instrumentação Agropecuária - cruvinel@cnpdia.embrapa.br

ABSTRACT

Agricultural soil tomography aims at investigating soil proprieties as water and solute transport, soil porosity, soil contents, root growing and humidity. For a better analysis about these proprieties, an image quality is required. The enhancement of tomographic images can be reached by the use of filters in their projections (signals) with the objective to reach a better signal/noise relation. Previous works focused on image filtering or in the use of filters specialized in Gaussian process estimation. These techniques not presented significant improvement in signal to noise relation and additionally have showed losses in image details. These projections have different types of noises affecting the image quality directly and omitting important details that can be recognized as if they were noise or fake details caused by noises. This paper presents formulations for the use of unscented Kalman filter with neural networks in a dual estimation filtering: a filter for state estimation and a filter for weight estimation with the objective of obtaining better quality in the signal / noise relation of tomographic projections. Besides the filter uses nonlinear functions, the square root technique also improves the performance and numerical stability compared with the basic unscented Kalman Filter. The use of neural network applied to the square-root unscented Kalman filter showed significant results, as high ISNR values together with an image where details are kept.

Keywords: Kalman filter, Artificial Neural Network, Tomography.

I. INTRODUCTION

Widely used in medical areas, the use of Computerized Tomography (CT) in soil science has been introduced by Petrovic, Siebert and Riek [1], Hainswoth and Aylmores [2] and by Crestana [3]. Petrovic has shown the possibility of using an X-ray computed tomography to measure the density of soil volumes, while Crestana has demonstrated that CT can solve problems related to studies of the physics of water in the soil. From these studies, it led to a project involving the development of a tomography to soil science [4] [5]. The use of the computer tomography is essential for the image reconstruction from projections.

The application of CT for the investigation of soil physics properties in grain and pore levels is important to the water and solute transport study in this environment, particularly in non saturate regions, as well as for the interaction investigations of soil and roots. Combined with other conventional techniques as neutrons probes, gravimetry, gamma and X-ray direct transmission, tracers, optical microscopy, electron microscopy scanning, mercury intrusion and other similar ones, it contributes greatly to resolve diverse problems of soil area. The results were obtained in a millimeter order scale, while various answers are expected in particle, macropore and micropore levels [6]. In the visualization of a tomographic image there is the presence of granularity, which is significant in the viewing of objects in low contrast. This granularity may be considered as a fake detail in image.

Besides, the use of X-ray computer tomography requires, as its application, the use of digital filters. They are necessary since the studied signal is represented discretely and due to the ability to treat an adaptive approach to promote a best filtering. One of them is the Kalman filter. This mathematical tool developed based on concepts such as (hidden) Markov chains [7], Bayesian estimation among others. It has the ability to obtain future and hidden states given the observation and to improve with the other techniques of estimation. In this paper is used as artificial neural networks, but can be applied either in genetic algorithms. These filters are seen as extensions of nonlinear filters and changes are made directly in the equations for filter measurement and correction.

The linear filtering main characteristic is the ability to make a prediction using a known linear function. For the discrete filter the translation matrix was used, where the difference from the future state and the current state is estimated. The observed value shall be the sum of these states after being corrected by the filter. The non-linear filtering can be made through the use of a nonlinear function for this estimation. This is done with the use of neural networks that promote a non-linear mapping and the use of the filter to estimate the neural network weights.

The Kalman filter is a mathematical tool widely used for statistical problems and is considered a good estimator for a large class of problems and an effective and useful estimator for other classes. In 1960, Rudolf Emil Kalman published an article describing a recursive solution to the problem of discrete data linear filtering. While there are several specific applications that are close to estimating an unknown state of a set of process measures, several of these methods do not inherently take into account the nature of the typical noise. For example, consider them working on a mapping for interactive computer graphics. While the requests for information vary with application, the key source of information is the same: estimate poses of measures that are derived from noisy electrical mechanical, inert, optical, acoustic or magnetic sensors. This noise is statistically typical in nature (or can be effectively modeled well), which leads to stochastic methods to address problems.

The techniques used in artificial intelligence and in estimation with Kalman filter are used to increase its filtering power to solve problems of higher orders. To determine the behavior of a function, it can use its own filter to perform a linear prediction or make a non-linear prediction using neural networks.

The main source of noise in CT images is quantum mottle, defined as the spatial and temporal statistical variation in the number of X-ray photons absorbed in the detector. Other types of noise present in CT images are the rounding errors in the program of reconstruction (noise of the algorithm) and the electronic noise attributed by the system displays. Electronic noise can originate in not ideal electronic devices, such as not pure resistors and capacitors, not ideal terminal contacts, current leakage transistors, Joule and can also be independent of the signal, such as external interference (electrical or even mechanical) [8] [9] [10] [11]. The low-pass filters and median are solutions to solve the problem of signal or noise, but there is loss of crucial information. Systems with different source noise do not have a solution with the use of filter. There is, therefore, the need for more use of filters complex that can be seen in [12] [13] [14], which also provide a comparison with a solution of using neural networks (pre-filter) with Discrete Kalman filter.

This paper is regarding to understand the use of unscented Kalman filter (UKF) and the algorithm used to separate a noise from a signal. This will be done by showing that the unscented Kalman filter with neural network is the best option for filtering. It will be an overview and specified after each equation of the algorithm.

The unscented Kalman filter is similar to the extended version [15]. The distribution of states is represented by a Gaussian random variable, but is now specified using a minimum of sampling point sets chosen carefully. The sampled points capture the true mean and covariance of random variable and when it propagates through a truly non-linear system, it captures the mean and covariance accurately to promote a third order estimation for any nonlinearity. Thus, this is done through the use of unscented processing.

An unscented processing (Unscented Transform) is a method to calculate the statistics of a random variable x (with dimension L), which can be understood as a noiseless free projection that, through a non linear function $y = g(x)$ results in an observed state or a noisy projection. Assuming x has mean $\bar{x}$ and covariance P_x. To calculate the statistics of y, it must form a matrix X with $2L+1$ sigma vectors *sigma* X_i (with weight W_i), according to the following:

$$X_i = \bar{x} \tag{1}$$

$$X_i = \bar{x} + (\sqrt{(L+\lambda)P_x})_i \text{, for } i = 1,\ldots, L \tag{2}$$

$$X_i = \bar{x} - (\sqrt{(L+\lambda)P_x})_i \text{, for } i = L+1,\ldots,2L \tag{3}$$

$$W_o^{(m)} = \lambda / (L+\lambda) \tag{4}$$

$$W_o^{(c)} = \lambda / (L+\lambda) + (1-\alpha^2+\beta) \tag{5}$$

$$W_i^{(m)} = W_i^{(c)} = 1/\{2(L+\lambda)\} \text{, for } i = 1,\ldots,2L \tag{6}$$

where $\lambda = \alpha^2(L+k) - L$ is a scalar parameter. The variable α determines the sigma points spreading around the mean $\bar{X}$ and it is ever a minimal positive value. *k* is a secondary scalar parameter that is equal to 0 for a single state and equal to $3-L$ for weight estimation and β is used to incorporate the distribution a priori knowledge *x* (for Gaussian distributions, $\beta = 2$ is optimal). $(\sqrt{(L+\lambda)P_x})_i$ is the i-th square root matrix line. These sigma vectors are propagated through non linear function

$$y_i = g(X_i) \text{ for } i = 0,\ldots,2L \tag{7}$$

and the y_i mean and covariance are approximate using sample mean and covariance of posteriors sigma points.

$$\bar{y} \approx \sum_{i=0}^{2L} W_i^{(m)} y_i \tag{8}$$

$$P_y \approx \sum_{i=0}^{2L} W_i^{(c)} \{y_i - \bar{y}\}\{y_i - \bar{y}\}^T . \tag{9}$$

Unscented Kalman filter algorithm

Sigma points calculation:

$$X_k^n = [\overset{a}{x}_{k-1} \ \overset{a}{x}_{k-1} \pm \sqrt{(L+\lambda)} P_{k-1}^a] \quad (10)$$

where X is the set of points with unscented transformation based on the mean and covariance *a priori*.

Preview equations:

$$\widehat{\bar{x}}_k = \sum_{i=0}^{2L} W_i^{(m)} x_{i,k|k-1}^x \quad (11)$$

where $W^{(m)}$ represents the set of sigma point weights used for true mean reconstruction.

$$P_k^- = \sum_{i=0}^{2L} W_i^{(c)} [X_{i,k|k-1}^x - \bar{x}_k][X_{i,k|k-1}^x - \bar{x}_k]^T \quad (12)$$

where $W^{(c)}$ represents the set of sigma point weights used for true mean reconstruction.

$$X_{k|k-1}^x = F(X_{k-1}^x, X_{k-1}^v) \quad (13)$$

where F is the function for the sigma propagation for state transitions.

Correction equations:

$$Y_{k|k-1} = H(X_{k-1}^x, X_{k-1}^n) \quad (14)$$

where H is the system function for sigma points generation of observation states Y.

$$\bar{y}_k = \sum_{i=0}^{2L} W_i^{(m)} Y_{i,k|k-1}^x \quad (15)$$

where y is the observed state estimation reconstructed for the sigma points.

$$P_{y_k y_k}^- = \sum_{i=0}^{2L} W_i^{(c)} [Y_{i,k|k-1} - \bar{y}_k][Y_{i,k|k-1} - \bar{y}_k]^T \quad (16)$$

$$P_{x_k y_k} = \sum_{i=0}^{2L} W_i^{(c)} [X_{i,k|k-1} - \bar{x}_k][Y_{i,k|k-1} - \bar{y}_k]^T \quad (17)$$

$$K = P_{x_k y_k} (P_{y_k y_k})^{-1} \quad (18)$$

where K is the Kalman gain obtained through the noise covariances.

$$x_k = \bar{x}_k + K(y_k - \bar{y}_k) \quad (19)$$

this equation represents the mean *a priori* correction and

$$P_k = P_k^- - K(P_{y_k y_k}) K^T \quad (20)$$

represents the covariance *a priori* correction.

This method differs from the general methods of sampling (Monte-Carlo methods such as particle filters), which require orders of magnitude with more sample points in an attempt to define and propagate the state (possibly non-Gaussian) distributions. The unscented approaches result in more hits for the third order for Gaussian inputs for all nonlinearities. For non-Gaussian inputs, approximations are more reliable, at least for a second order, with the success of moments for third order or higher orders determined by the choices of α and β .

The unscented Kalman filter is a direct extension of unscented transformed for the equation recursive estimation

$$x_k = (\text{ prediction of } x_k) + K_k \cdot [y_k - (\text{ prediction of } y_k)] \tag{21}$$

where the state of random variable is redefined with the concatenation of original states and noise:

$$x_k^a = [x_k^T v_k^T n_k^T]^T . \tag{22}$$

The selection of sigma points is applied for a new random variable state to selection to calculate the corresponding sigma matrix x_k^a . The unscented Kalman filter equations are given below. They do not need to calculate Jacobian or Hessians matrices, in addition, the calculation total numbers are the same of extended filters

. The Kalman filter was originally designed to solve a problem of state estimation, and has been used in applications related to nonlinear controls that require feedback from the states. In these applications the dynamic model is a physically based parametric model, which assuming is known.

Due to numerical instability related to the filter noise, and the use of the Cholesky factorization to determine the square root of probability matrix, Rudolph van der Merwe and Eric A. Wan have developed the square-root unscented Kalman filter (SRUKF) [16], which allows better control variance matrix values, bypassing the problem of becoming a negative or indefinite matrix. This new filter also provides an improvement in performance, leaving the unscented Kalman filter with the same order of complexity of the extended filter.

As the original unscented Kalman filter, the square root filter is initialized by calculating the square root of covariance matrix states by the Cholesky factorization:

$$S_0 = chol\{E[(x_0 - \hat{x}_0 \wedge)(x_0 - \hat{x}_0 \wedge)^T]\} \tag{23}$$

However, the spread factor and the update of Cholesky is then made in subsequent iterations to directly form the sigma points. In the equation below, the update time of the Cholesky factor is calculated by using a QR decomposition of the matrix composed of the weight of the propagated sigma points and the square root of covariance matrix of the additive noise case:

$$S_k^- = qr\{[\sqrt{W_1^{(c)}}(X_{1:2L,k|k-1}^* - \hat{x}_k^-)\sqrt{R^v}]\} \tag{24}$$

A subsequent update of Cholesky (or regression) in the equation below is needed since the weight zero is perhaps negative:

$$S_k^- = cholupdate\{S_k^-, X_{0,k}^* - \hat{x}_k^-, W_0^{(c)}\} \tag{25}$$

These two steps replace the time update. They are also used in the calculation of the Cholesky factor, the error covariance of the observation:

$$S_{\bar{y}k} = qr\{[\sqrt{W_1^{(c)}}(Y_{1:2L,k} - \hat{y}_k^-)\sqrt{R^n}]\} \tag{26}$$

$$S_{\bar{y}k} = cholupdate\{S_{\bar{y}k}, Y_{0,k} - \hat{y}_k^-, W_0^{(c)}\}\ . \tag{27}$$

Unlike the way in which the gain of Kalman filter is calculated in standard unscented, using two inversions:

$$K_k(S_{yk}S_{yk}^T) = Px_k y_k \tag{28}$$

Since it is square and triangular, efficient replacements can be used to solve it directly without the need for an inversion of the matrix. Finally, the Cholesky factoration update of the covariance factor of the state in the equation below is calculated by applying sequential Cholesky regressions

$$S_k = cholupdate\{S_k^-, U, -\} \tag{29}$$

The vectors are the columns of the equation regression 19. This update replaces the rear equation 20

$$U = K_k S_{yk} \tag{30}$$

With the knowledge of non-linear function of the process and a Kalman filter that supports non linear functions is possible to get a significant improvement in the signal. One solution is to use a neural network to promote a better function of the mapping process, reducing the noise present in the projections. For an estimation of the weights of the neural network together with the estimates of the states, we can use two methods of filtering: the estimation and dual estimation. These arrangements for determining the filtering initial weights are known, the next state is obtained in a linear mapping with the previous one.

Details of unscented Kalman filter implementations and modeling are shown in section 2. Section 3 presents a comparison of the results obtained by the filters. Finally, section 4 presents the conclusion.

II. METHODOLOGY

The equipment utilized is a first generation mini-tomograph scanner developed at Embrapa Agricultural Instrumentation. The mini-tomograph data acquisition process provides a matrix with the sample values of projections. For the modeling process, it considers a matrix row that, by convention, is named sum ray. This signal is composed of various incidences with variable and non deterministic values, whose amplitude is given by

$$I_m[n] = I_0 e^{-\mu d}, \tag{31}$$

where d is the distance traveled by the photon ray within the evidence body, μ is the attenuation coefficient, I_o is the free beam counting and I_m is the projection n attenuated beam .

This allows a filtering with *a priori* knowledge only in the previous variable. Thus, the transference and system matrices are reduced as:

$$\begin{bmatrix} P_{\theta_i}[n] \\ I_{m-1}\delta(n-m-1) \end{bmatrix} = \begin{bmatrix} 1 & 1 \\ 0 & 1 \end{bmatrix} \begin{bmatrix} I_m \delta(n-m) \\ I_{m-1}\delta(n-m-1) \end{bmatrix} \tag{32}$$

$$P_{\theta_i}[n] = \begin{bmatrix} 1 & 0 \end{bmatrix} \begin{bmatrix} P_{\theta_i}[n] \\ I_{m-1}\delta(n-m-1) \end{bmatrix} \tag{33}$$

Matrix [1 0] corresponds to matrix H of the system equation, which allows to power or to hide the observation states according to hidden Markov chains. This allows the filter to estimate states that are not visible outside the system.

The Kalman filter can be a nonlinear function and train parameters (weights). There is then the possibility of using a mapping function with neural networks where the filter trains the neurons and moves to a stable system where the weights are estimated and the mapping function has the lowest error rate possible. This filter allows working with higher orders (with the accuracy equivalent to the expansion of third order Taylor series), while the filter, in its extended form, works only with second order functions.

With the knowledge of a non-linear function of the process and a Kalman filter that supports linear functions to get a significant improvement in the signal. One solution is to use a neural network to promote a better function of the mapping process, reducing the noise present in the projections. For a weight estimation of the neural network together with the states estimation, it is possible to use two methods of filtering: the state estimation and the dual estimation.

The use of Hidden Markov Chains model to estimate weights of a neural network arose from the need to obtain an estimator for the Kalman filter that could map the nonlinear functions efficiently and better than the process of linearization (applied in translations) and merge other functions without the need to create several states to map a single behavior. These arrangements for determining the filtering initial weights are known, the next state is obtained in a linear mapping with the previous state. Thus, it has:

$$x_{k+1} = f(x_k, W_k, v_k) \tag{34}$$

Then, a Kalman filter to estimate the states and a Kalman filter to estimate the weights are used. This filtering allows the application in a system where the dynamics of status is unknown or chaotic (non-deterministic). Then it has a filtering system with dual estimation that can be written as:

$$x_{k+1} = f(x_k, W_k, v_k) \tag{35}$$

$$z_k = h(x_k, n_k) \tag{36}$$

$$W_{k+1} = \eta W_k \tag{37}$$

$$y_k = g(x_k, W_k, m_k) \tag{38}$$

$$e_k = x_k - y_k \tag{39}$$

It can be used the two forms of Kalman filter for nonlinear systems to compose the dual. Despite being a more complete estimate, it is still prone to errors since the estimation of the signal observed is approximate.

III. RESULTS AND DISCUSSION

As the Kalman filter works on a white noise process it takes up the value of variance Q, which determines the degree of confidence in the process. To measure the quality of filtering, the ISNR variance was used based on the windows (ROIs) in reconstructed images. A negative ISNR (Improvement in Signal Noise Ratio) indicates a loss of detail or deformation (presence of artifacts) in the final image. For the heterogeneous phantom, five windows (ROIs) were used, where the presence of a negative value or a decrease of ISNR values indicate a lower quality of filtering. In the homogeneous phantom, a ROI of 42 X 28 pixels was used and in the heterogeneous phantom, five ROIs of 14 X 11 pixels were used to quantify the results obtained with the filters. For the last, a soil sample is used to validate the results. TABLE 1 presents test results to verify the relationship between ISNR and the quality of the signal and the image reconstructed with SRUKF. TABLE 2 shows the results of test ISNR values and the results of applying the filter with artificial neural network.

TABLE 1 - Results obtained with the unscented Kalman filter and phantoms for calibration. The (1) is defined as homogeneous phantom and the (2) is defined as heterogeneous phantom.

Q=1	**Max ISNR (dB)**					
	(1)	**(2)**				
R=0.01	-0.57	4.52	4.43	4.63	1.82	3.96
R=0.5	-0.81	4.52	4.43	4.63	1.82	3.96
R=0.8	-0.59	4.52	4.43	4.63	1.82	3.96
R=1	-1.88	4.52	4.43	4.63	1.82	3.96
R=5	-2.76	4.52	4.43	4.63	1.82	3.96
R=10	-0.17	4.52	4.43	4.63	1.82	3.96
R=15	-2.40	4.52	4.43	4.63	1.82	3.96
R=20	-0.40	4.52	4.43	4.63	1.82	3.96

By analyzing the values of the table, it may experience a drop in the ISNR homogeneous phantom due to the presence of peaks in the image. These peaks may be originated of the reconstruction algorithm itself or even by the presence of other mechanical noises. The filter is stable because the Poisson noise is more influential than the white noise in high counts of photons.

The best result with a homogeneous phantom was with the system variance value of 10, while the heterogeneous phantom was stable for any value of the variance. The system filtering of white noise was effective for both samples and the drop in value of ISNR in homogeneous phantom is due to the estimation of future states of the filter match the noise in the samples. The results obtained by applying the filter to the phantoms can be seen in FIGURE 1.

TABLE 2 - Results obtained with the unscented Kalman filter with neural networks and phantoms for calibration. . The (1) is defined as homogeneous phantom and the (2) is defined as heterogeneous phantom.

Q=1	**Max ISNR (dB)**					
	(1)	**(2)**				
R=0.01	4.75	2.31	1.91	2.35	1.24	1.67
R=0.5	6.63	5.11	4.31	5.34	2.81	3.86
R=0.8	6.77	6.53	5.64	6.86	3.85	5.03
R=1	6.73	7.37	6.31	7.74	4.34	5.68
R=5	7.62	10.86	8.69	11.13	2.30	8.38
R=10	7.91	13.92	10.88	13.76	-0.73	12.52
R=15	7.65	16.73	12.66	15.84	-1.85	16.14
R=20	7.05	19.01	14.13	17.38	-2.47	14.95

Noting the filtered projections, it is possible a more consistent and stable filtering. Looking at the variance of pixel values in the reconstructed image of the homogeneous phantom, we find a concentration of values in a lower range, even with the presence of pixels with different values (darker). The heterogeneous phantom showed better stability, the samples are well defined within the body studied. As the filter can accurately estimate the noise affecting the states of the observation process and the results show better details. A multi-layer perceptron neural network is used with 2 neurons in a hidden layer and 1 neuron in an output layer.

The filter with unscented estimation proved to be stable for the homogeneous phantom, with little different values. The same result was not reached with the heterogeneous phantom in that it is possible to repair the distortion and loss of detail due to the simplicity of the neural network applied.

There was an improvement in higher values obtained by the filter, due to the efficiency of the unscented algorithm. The higher values represent a greater fall in the variance value in the regions of interest, demonstrating a better filtering.

The tests with the unscented filter and neural networks provided a better result than the extended filter, despite the distribution of values of ROIs be differentiated. This delay is due to the convergence of the network signal.

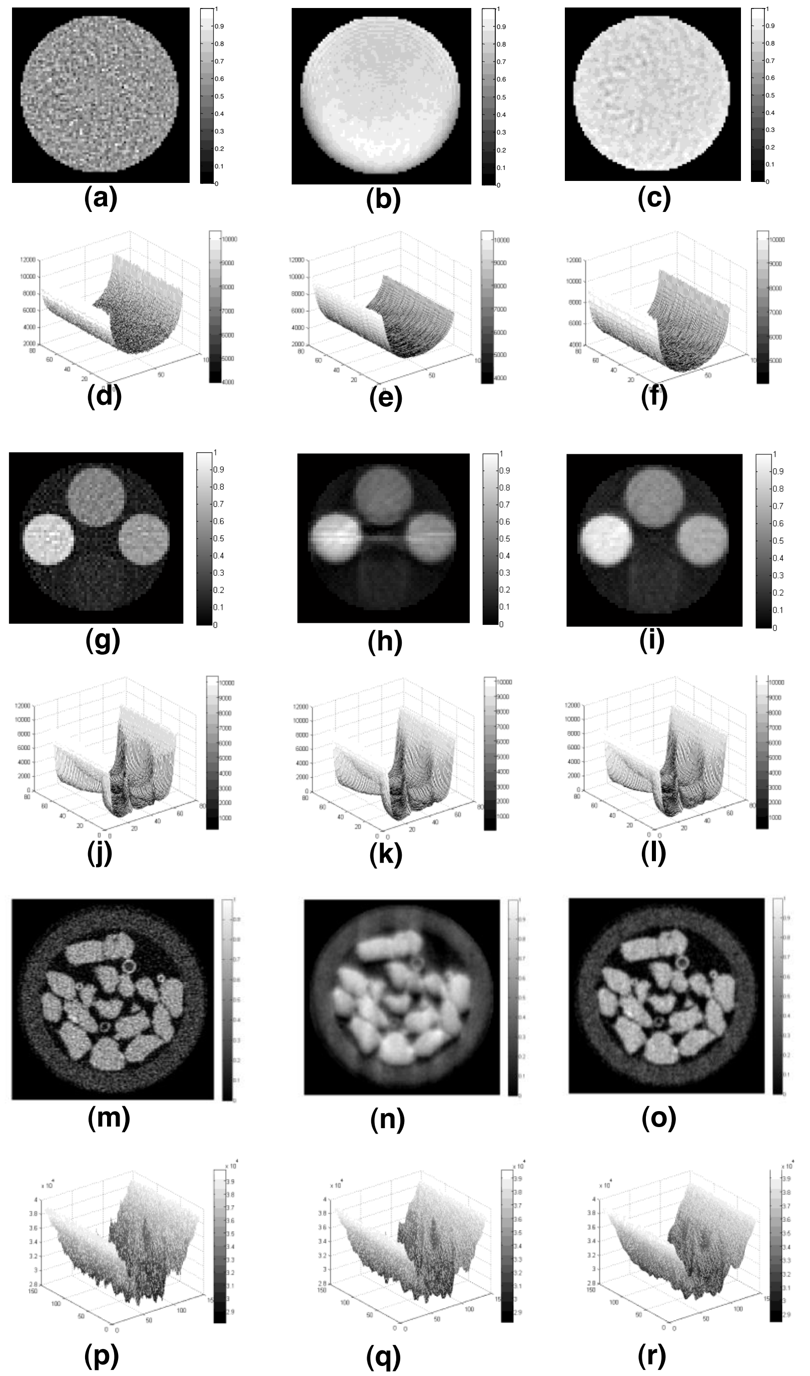

FIGURE 1 – Results using the square-root Kalman filter. In the first column the original projections are represented, together with their respective reconstructed images. In the second column, it is possible to see the obtained results using a canonical observed model and last column shows the use of the filter in dual estimation mode.

The results were as expected and have, to some extent, the same visual results for the implementation of unscented and basic filters, proving that the characteristics of Poisson noise can be mapped by a neural network, where the complexity to understand the process of equations deeply can be replaced by an iterative intelligent system, able to find new sensor features over time (difference in temperature, equipment aging and new mechanical structures). The results with soil sample show the dual estimation can reach a better image due to the presence of image details and no blurring effects in the sand grains.

IV. CONCLUSION

The unscented Kalman filter uses the resources for the creation of sigma points in the mean and around it, making a better mapping of the variance behavior excluding the need for calculations with matrices of linearization. The filter implemented in this work has several feature clusters: Increased use of covariance, which allows working with the signal, noises and process and system noise variances at the same time, allowing noise estimation, something that does not happen with the other Kalman filters; Use the type of filter to square root, which using the Cholesky factoration allows greater stability of the filter concerning the noise and a gain in the filter order; Freedom to use the algorithm without the need for a priori knowledge of the response functions;Accuracy equivalent to third-order functions without the need for neural networks.

Despite the use of a translation function be something simple and perhaps more suitable for a range of problems, due to the processing time and memory required, the Kalman filter with neural network replaces the old algorithms with these techniques due to the minimal use of layers and number of neurons in these layers. In addition, the use of the dual estimation modifies the initial intense training, what not always guarantees the convergence and adaptability to a better result and proves that a translation function implemented in the model of hidden Markov chains is not so efficient as the use of this model to identify the weights.

As the unscented Kalman filter, it allows the mapping functions for the use of higher orders through the mapping of the mean and variances by the sigma points, without the use of linearization by Jacobian and Hessian matrices.

The use of neural networks with this filter type allows mapping any function, with precise estimation of results. Additionally, by checking the results of the unscented Kalman filter with neural networks in phantoms, it was possible to observe the efficiency of the filter to adapt to the chaotic features, such as heterogeneities normally present in real samples.

As a pre-filtering, maintaining details in an image should be the most important objective.

V. REFERENCES

[1] A. M. Petrovic, J.E. Siebert, P.E. Rieke, “Soil bulk analysis in three dimensions by computed tomographic scanning”, *Soil Sci. Soc. Am. J.*, n.46, p.445-450, 1982.

[2] J. M. Hainsworth, L. A. G. Aylmore, “The use of the computed-assisted tomography to determine spatial distribution of soil water content”, *Aust. Journal Soil Res.*, N. 21, p.1435-1443,1983.

[3] S. Crestana, “A Tomografia Computadorizada com um novo método para estudos da física da água no solo”, *São Carlos, USP, 140 p.*, 1985.

[4] P. E. Cruvinel, ”Minitomógrafo de raios X e raios gama computadorizado para aplicações multidisciplinares”. *Campinas, UNICAMP, 329 p.,* 1987.

[5] P. E. Cruvinel; R. Cesareo; S. Crestana; S. Mascarenhas, “X and γ-ray computerized minitomograph scanner for soil science”, *IEEE Transactions on Instrumentation and Measurement*, V.39, N.5, p.745-750, October, 1990.

[6] S. Crestana, “Técnicas recentes de determinação de características do solo.”, *Reunião brasileira de manejo e conservação do solo e da água*, vol. 10, 1994, Abstracts, Florianópolis: Sociedade Brasileira de Ciência do Solo, p86-97, 1994.

[7] R. E. Kalman,"A new approach to Linear Filtering and Prediction Problems." *Transaction of the ASME - Journal of basic Engineering*, 1960.

[8] A. J. Duerinckx, A. Macocski, “Polychromatic Streak Artifacts in Computed Tomography Images”, *J.Comput. Assist. Tomogr., 2.481,* 1978.

[9] P. M. Joseph, R.D. Spital, “A method for correction bone-induced artifacts of CT scanners”, 1978.

[10] G. S. Ibbott, “Radiation therapy treatment planning and the distortion of CT images”, *Med. Phys, 7:261*,1980.

[11] L. F. Granato, “Algoritmo adaptativo para a melhoria em imagens tomográficas obtidas em múltiplas energias”, *São Carlos, UFSCar, 135 p.,* 1998.

[12] M. A. M. Laia, P. E. Cruvinel, “Filtragem de projeções tomográficas utilizando Kalman Discreto e Rede Neurais”, *IEEE América Latina,vol. 6, ed. 1, march*, 2008.

[13] M. A. M. Laia, P. E. Cruvinel, A. L. M. Levada, “Filtragem de projeções tomográficas da ciência do solo utilizando transformada de Anscombe e Kalman”, *DINCON’07, São José do Rio Preto*, 2007.

[14] M. A. M. Laia, P. E. Cruvinel. "Filtragem de projeções tomográficas do solo utilizando Kalman e Redes Neurais numa estimação conjunta", *DINCON'08, Presidente Prudente,* 2008.

[15] S. J. Julier, J. K. Uhlmann, "A new extension of Kalman filter to nonlinear systems." *Symp. Aerospace/Defense Sensing, Simul. and Controls*, 1997.

[16] R. van der Merve, E. A. Wan. "The square-root unscented Kalman Filter for state and parameter-estimation." *Acoustics, Speech, and Signal Processing, 2001. Proceedings. (ICASSP '01). 2001 IEEE International Conference on*, 2001: 3461-3464.